AMERICAN ACADEMY OF OPHTHALMOLOGY®

Early Sign of Retinal Neovascularization Evolution in Diabetic Retinopathy

A Longitudinal OCT Angiography Study

Kotaro Tsuboi, MD,[1,2] Mehdi Mazloumi, MD, MPH,[1] Yukun Guo, MS,[1] Jie Wang, MS,[1,3] Christina J. Flaxel, MD,[1] Steven T. Bailey, MD,[1] David J. Wilson, MD,[1] David Huang, MD, PhD,[1] Yali Jia, PhD,[1,3] Thomas S. Hwang, MD[1]

Purpose: To assess whether the combination of *en face* OCT and OCT angiography (OCTA) can capture observable, but subtle, structural changes that precede clinically evident retinal neovascularization (RNV) in eyes with diabetic retinopathy (DR).

Design: Retrospective, longitudinal study.

Participants: Patients with DR that had at least 2 visits.

Methods: We obtained wide-field OCTA scans of 1 eye from each participant and generated *en face* OCT, *en face* OCTA, and cross-sectional OCTA. We identified eyes with RNV sprouts, defined as epiretinal hyperreflective materials on *en face* OCT with flow signals breaching the internal limiting membrane on the cross-sectional OCTA without recognizable RNV on *en face* OCTA and RNV fronds, defined as recognizable abnormal vascular structures on the *en face* OCTA. We examined the corresponding location from follow-up or previous visits for the presence or progression of the RNV.

Main Outcome Measures: The characteristics and longitudinal observation of early signs of RNV.

Results: From 71 eyes, we identified RNV in 20 eyes with the combination of OCT and OCTA, of which 13 (65%) were photographically graded as proliferative DR, 6 (30%) severe nonproliferative DR, and 1 (5%) moderate nonproliferative diabetic retinopathy. From these eyes, we identified 38 RNV sprouts and 26 RNV fronds at the baseline. Thirty-four RNVs (53%) originated from veins, 24 (38%) were from intraretinal microabnormalities, and 6 (9%) were from a nondilated capillary bed. At the final visit, 53 RNV sprouts and 30 RNV fronds were detected. Ten eyes (50%) showed progression, defined as having a new RNV lesion or the development of an RNV frond from an RNV sprout. Four (11%) RNV sprouts developed into RNV fronds with a mean interval of 7.0 months. Nineteen new RNV sprouts developed during the follow-up, whereas no new RNV frond was observed outside an identified RNV sprout. The eyes with progression were of younger age ($P = 0.014$) and tended to be treatment naive ($P = 0.07$) compared with eyes without progression.

Conclusions: Longitudinal observation demonstrated that a combination of *en face* OCT and cross-sectional OCTA can identify an earlier form of RNV before it can be recognized on *en face* OCTA.

Financial Disclosure(s): Proprietary or commercial disclosure may be found in the Footnotes and Disclosures at the end of this article. *Ophthalmology Science 2024;4:100382*

Supplemental material available at www.ophthalmologyscience.org.

Diabetic retinopathy (DR) is the leading cause of preventable blindness in the working-age population worldwide.[1–3] Retinal neovascularization (RNV) is the key clinical feature of proliferative diabetic retinopathy (PDR) that predisposes the patient to severe vision loss due to vitreous hemorrhage or tractional retinal detachment. An early detection of RNV and prompt treatment can prevent disease progression and subsequent vision loss.[4] In the ETDRS, the Diabetic Retinopathy Study Scale provides the probability of progression of PDR.[5] Intraretinal microvascular abnormality (IRMA) is one of the hallmarks of end-stage nonproliferative diabetic retinopathy (NPDR), and the severity of IRMA has been shown to be a risk factor for the progression into PDR.[6]

Prior studies demonstrated structural and angiographic changes at the location of IRMA.[7–10] Lee et al demonstrated the OCT features differentiating RNV from IRMA.[7] Longitudinal observation with structural cross-sectional OCT showed that IRMA outpouching of the internal limiting membrane (ILM) gradually increased in size and

https://doi.org/10.1016/j.xops.2023.100382
ISSN 2666-9145/23

eventually breached the ILM, confirming RNV. Russel et al also reported the longitudinal progression of RNV from IRMA using OCT angiography (OCTA).[8] Serial OCTA images illustrated the intraretinal flow signals at the location of IRMA extended to the RNV, suggesting that IRMA could be a precursor lesion of RNV and that the combination of structural OCT and OCTA can be useful for detecting the early development of RNV. However, RNV originates not only from IRMA but also from retinal capillary beds,[11–13] postcapillary venules,[12,13] and retinal veins.[12–14]

Recently, we have identified presumed glial sprouts as an early biomarker for detecting RNV with serial OCTA in an eye with branch retinal vein occlusion.[15] We observed that the presumed glial sprout, seen as hyperreflective tissues on *en face* OCT, emerged on the retinal vessel 6 months before RNV development. The longitudinal observations illustrated that the presumed glial proliferation increased in size, and the flow signal extended toward the vitreous cavity, eventually developing into RNV at the location of preexisting glial proliferation. Because *en face* OCT can overview abnormal structures on the entire plane of the retinal surface, the combination of *en face* OCT and OCTA may be useful for detecting the early sign of RNV formation.

The purpose of this study was to assess whether the combination of *en face* OCT and OCTA can capture observable but subtle, structural changes that precede clinically evident RNV in eyes with DR. We conducted a longitudinal observation study including eyes from a prospective DR cohort with at least 2 visits. We analyzed all lesions with abnormal structures on *en face* OCT with flow signal breaching the ILM on cross-sectional OCTA to characterize the early signs of RNV.

Methods

This retrospective cohort study comprises 2 prospective OCT/OCT angiography (OCTA) studies of DR (NIH R01 EY027833) performed at the Casey Eye Institute, Oregon Health Science University. The details of the studies have been previously published.[16–20] The study adhered to the tenets of the Declaration of Helsinki and complied with the Health Insurance Portability and Accountability Act of 1996. The institutional review board of Oregon Health Science University approved the study. All participants provided a written informed consent to participate in the OCT/OCTA studies.

The study included eyes with DR that underwent wide-field OCTA imaging protocol at least twice, with a minimum interval of 5 months, from December 19, 2017, to February 25, 2022. Data analysis was performed in April 2022. The study excluded pregnant or lactating women, those unable to consent or cooperate with OCT or OCTA scans, or those with the presence of significant nondiabetic ocular diseases such as age-related macular degeneration. Only 1 eye of each participant was included in the study.

All participants underwent ETDRS protocol for visual acuity, intraocular pressure measurement, slit-lamp biomicroscopy, and indirect binocular ophthalmoscopy. Standard 7-field ETDRS color fundus photography was performed at the baseline visit, and a retinal specialist (T.S.H.) assessed the severity of DR based on standard 7-field ETDRS color fundus photographs using the ETDRS severity scale. OCT angiography findings were not considered in the grading.

The current study used 2 commercially available OCTA devices to generate a montage wide-field OCTA scan. A 70-kHz spectral-domain OCT (Avanti; OptoVue) was used between December 19, 2017, and December 13, 2019, and a 120-kHz spectral-domain OCT (Solix; OptoVue) was used from January 15, 2020, to February 25, 2022. The scan protocol for Avanti was 3 6- × 6-mm high-definition OCTA scans (400 × 400 sampling positions) centered on the fovea, the disc, and the point 5 mm temporal to the fovea, generating a 15- × 6-mm montage OCTA. The scan protocol for Solix was 4 9- × 9-mm (600 × 600 sampling positions) OCTA scan patterns centered on points superotemporal to the fovea, superonasal to the fovea, inferotemporal to the fovea, and inferonasal to the fovea, generating an approximately 17- × 17-mm montage OCTA. Despite the different fields of view between the OCTA devices, both montage images have the same sampling density (15 μm/A-line).

A custom segmentation that optimized identification of RNV was used, with distinct custom segmentations for *en face* OCT and *en face* OCTA. The vitreoretinal interface slab has been described in the literature to optimize the visualization of RNV in OCTA.[12,21–23] In this study, for *en face* OCT, the vitreoretinal interface slab was bounded by the internal limiting membrane (ILM) and the position 30 μm anterior to the ILM. For *en face* OCTA, the slab was bounded by the ILM and the position 300 μm anterior to the ILM (Fig S1, available at www.ophthalmologyscience.org).

We defined RNV based on the flow signal above the ILM seen on cross-sectional OCTA corresponding to epiretinal hyperreflective material (EHM) on *en face* OCT or abnormal flow signal on *en face* OCTA (Fig 2). Further, based on the morphology, we divided the RNV lesions into RNV sprouts and RNV fronds (Table 1, Fig 3). Retinal neovascularization sprouts were defined as EHM on *en face* OCT with flow signals breaching the ILM on the cross-sectional OCTA without recognizable RNV on *en face* OCTA; and RNV fronds were defined as recognizable abnormal vascular structures on the *en face* OCTA. We did not differentiate IRMA with outpouching of the ILM from the IRMA with breaching of the ILM as proposed by Lee et al[7]. Intraretinal microvascular abnormality was defined as having dilated capillaries detected by *en face* OCTA with entire retinal slab but lack of structural change on the retinal surface by structural *en face* OCT and the corresponding cross-sectional OCT (Table 1). If abnormal structural changes (EHM on *en face* OCT) with flow signal were detected, we classified them into RNV spouts. If a follow-up scan disclosed any abnormalities, we examined all previous scans at the exact location registered based on superficial *en face* OCTA to determine whether the RNV was new or preceded by an abnormality. We evaluated the progression of RNV qualitatively. When a new RNV lesion or the development of an RNV frond from an RNV sprout was identified from the longitudinal observation, we defined this as progression.

Two trained graders (K.T. and M.M.) evaluated all RNV-suspected lesions using a combination of *en face* OCT, *en face* OCTA, and cross-sectional OCTA generated by commercially available software (ReVue, OptoVue, version 2018.1.1.63; and Solix ReVue, OptoVue, version 2019 V1.0.1.1). A senior grader (T.S.H.) resolved any discrepancies between graders. We assessed intergrade agreement on 40 montage scans from 20 participants using the intraclass correlation coefficient (ICC).

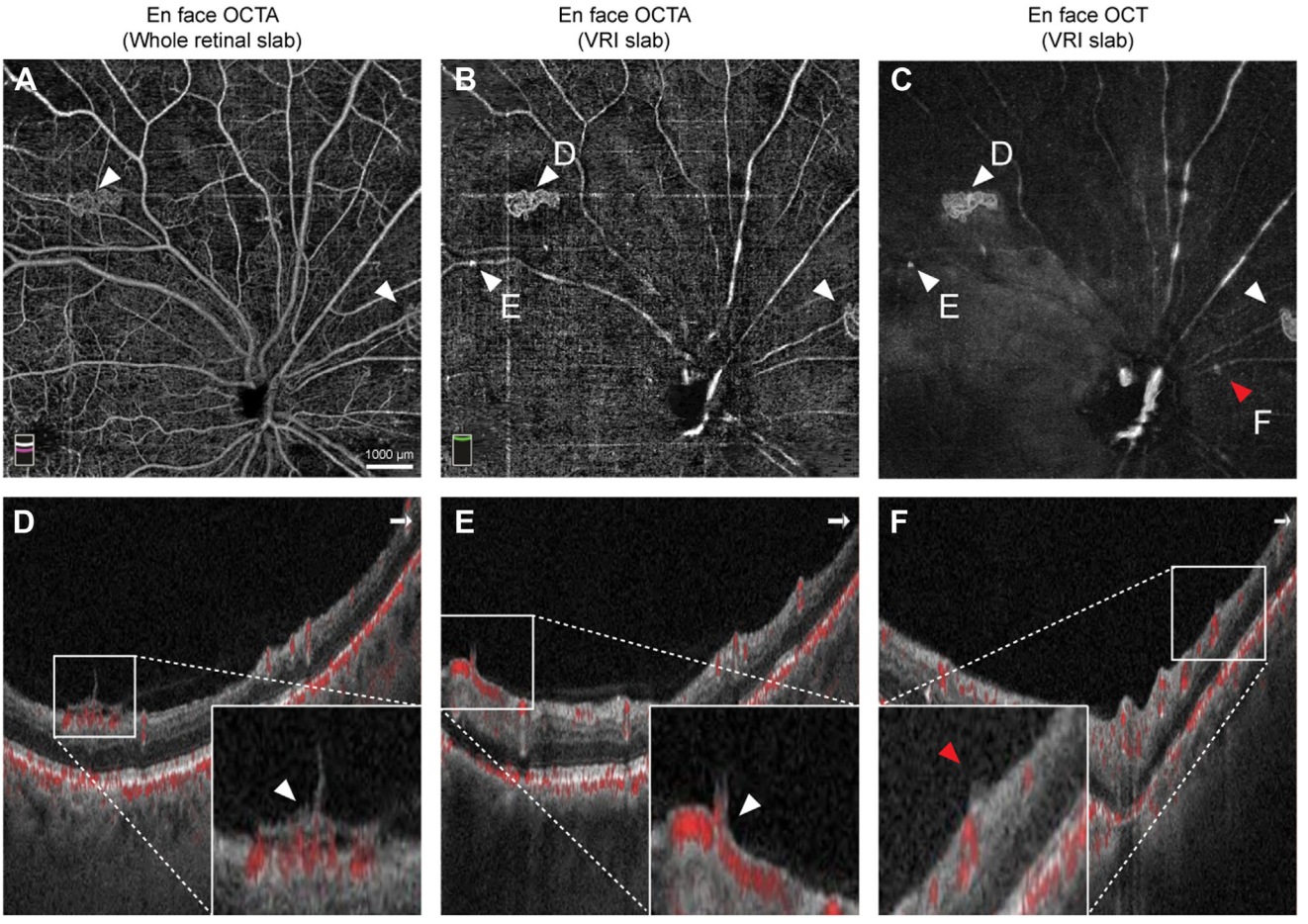

Figure 2. Four different image modalities from a single 9- × 9-mm OCT angiography (OCTA) scan were utilized for detecting retinal neovascularization (RNV). **A,** *En face* OCTA with entire retinal slab illustrated 2 RNV lesions (white arrows). **B,** *En face* OCTA with the vitreoretinal interface (VRI) slab bounded by the internal limiting membrane (ILM) and positioned 300 µm anterior, illustrated 3 RNV lesions (white arrows), and (**C**) *en face* OCT with a slab bounded by the ILM and positioned 30 µm anterior to the ILM toward the vitreous cavity, shows 4 areas of epiretinal hyperreflective material (EHM) (white arrows and red arrow). Abnormal flow breaching the ILM is confirmed at the location of RNV (**D, E**) on the corresponding cross-sectional OCTA. **C,** An EHM labeled F on *en face* OCT does not have any flow signal on the corresponding cross-sectional image (**F**), indicating that this is not an RNV lesion. Three RNV lesions are identified in this scanned area.

Table 1. Morphological Characteristics of Retinal Neovascularization

	Findings			
	En Face *OCT with VRI Slab*	En Face *OCTA with VRI Slab*	*Cross-sectional OCT*	*Cross-sectional OCTA*
IRMA	No abnormality	No abnormality*	No abnormality	Flow signals below the ILM
RNV sprout	Epiretinal hyperreflective material	Indistinct flow signal	Medium- to hyper- reflective pyramid-shaped abnormal tissue emerging on the retinal surface	Flow signals above the ILM connected to the retinal vasculature
RNV frond	Hyperreflective vascular structures	Vascular pattern flow signal	Increased epiretinal tissues	Vascular patten flow signal above ILM level

ILM = internal limiting membrane; IRMA = intraretinal microvascular abnormalities; OCTA = OCT angiography; RNV = retinal neovascularization; VRI = vitreoretinal interface.
*Note: *en face* OCTA with entire retinal slab illustrates dilated capillaries.

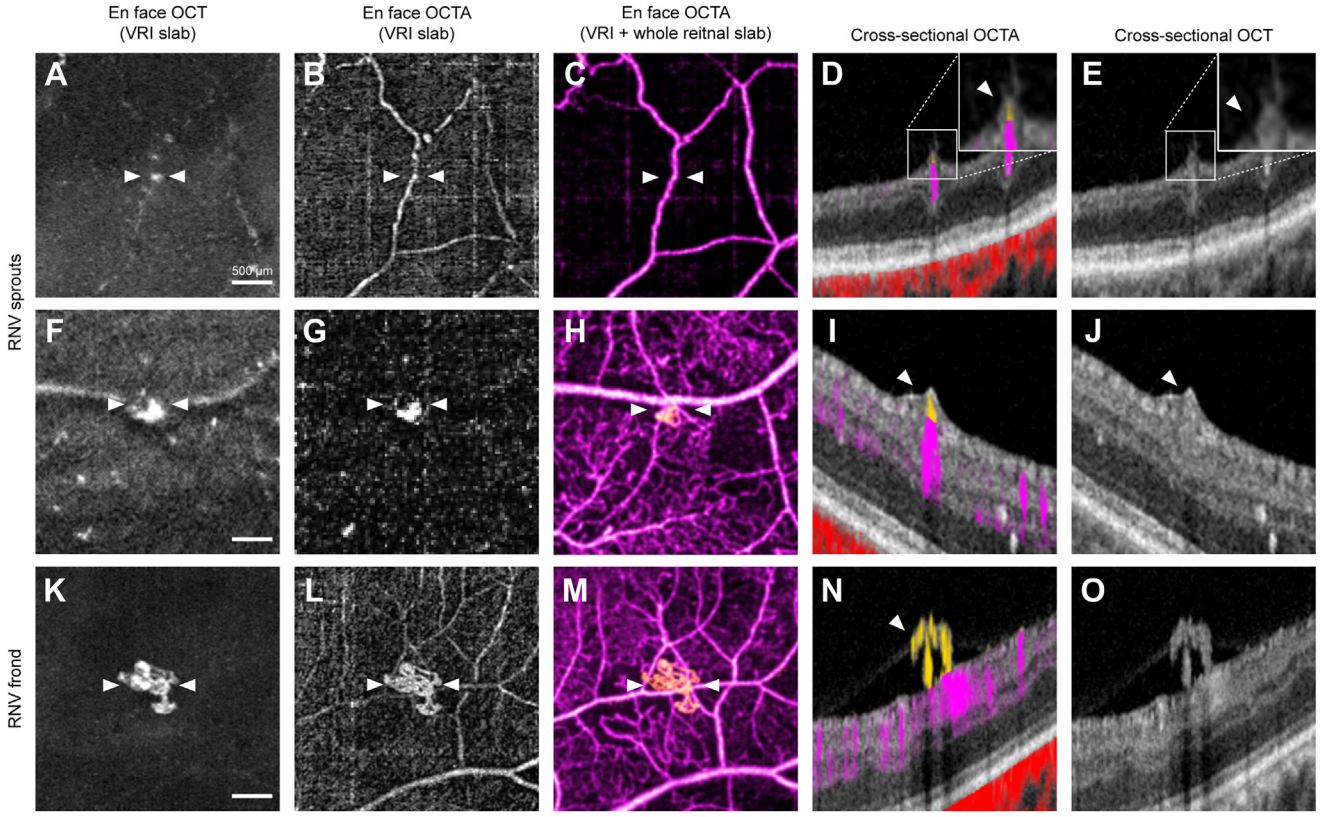

Figure 3. Classification of retinal neovascularization (RNV). **A–O,** The first and second rows show RNV sprouts. *En face* OCT (**A, F**) shows RNV sprouts as foci of epiretinal hyperreflective material (EHM) with flow signal above the internal limiting membrane (ILM) (orange vs. magenta for flow below the ILM) on cross-sectional OCT angiography (OCTA) (**D, I**). The cross-sectional OCT illustrates the pyramid-shaped proliferation emerging on the retinal vessels (**E, J**). However, the abnormal flow signal either cannot be detected (**B, C**) or is not distinct as a vascular structure (**G, H**) on *en face* OCTA. **K–O,** The bottom row shows an RNV frond, which is recognizable as a vascular network on *en face* OCT (**K**) and OCTA (**L, M**) with a clear flow signal above the ILM on the cross-sectional OCTA (**N, O**).

Descriptive statistics included the mean, standard deviation (SD), 95% confidence interval (CI), and percentages where appropriate. Normality was assessed by a normal probability plot and the Shapiro–Wilk test. All analyses were conducted using JMP version 13.1.0 (SAS Institute, Inc.) and GraphPad Prism (GraphPad Software). All P values were from 2-sided tests, and results were deemed statistically significant at $P < 0.05$.

Results

We initially reviewed a total of 71 eyes (PDR, 13 eyes; severe NPDR, 22 eyes; moderate NPDR, 19 eyes; mild NPDR, 17 eyes) with 226 wide-field OCTA scans. The mean (SD) follow-up duration was 13.1 (8.2) months (95% CI, 7.3–18.9 months), and the mean (SD) number of visits was 3.3 (1.2) visits (95% CI, 2.5–4.1 visits). Of these eyes, we found 20 eyes (28%) with RNV, of which 13 (65%) were photographically graded as PDR, 6 (30%) as severe NPDR, and 1 (5%) as moderate NPDR. Of the eyes with RNV, 11 (55%) were treatment-naive, defined as no previous panretinal photocoagulation or anti-VEGF injections. Patient characteristics of these 20 eyes are summarized in Table 2. The 2 graders had a high level of agreement on the diagnosis of RNV (ICC for RNV, 0.96), as well as the

Table 2. Demographic and Clinical Characteristics of the Eyes with Retinal Neovascularization

Parameters	(n = 20)
Age, yrs (SD) [95% CI]	53.5 (12.3) [47.7–59.2]
Sex, n (male/female)	11/9
Most recent HbA1c, % (SD) [95% CI]	8.0 (2.3) [6.8–9.1]
Duration of DM, yrs (SD) [95% CI]	21.7 (12.4) [15.9–27.5]
Type 1 DM, n (%)	10 (50)
Follow-up duration, mos (SD) [95% CI]	15.5 (10.8) [10.4–20.6]
OCTA scans, n (SD) [95% CI]	3.4 (1.2) [2.8–3.9]
DR stage	
Mild NPDR, eyes (%)	0 (0)
Moderate NPDR, eyes (%)	1 (5.0)
Severe NPDR, eyes (%)	6 (30.0)
PDR, eyes (%)	13 (65.0)
Treatment naive, eyes (%)	11 (55)
Previous treatment	
Panretinal photocoagulation, eyes	4
Intravitreal VEGF injection, eyes	5

CI = confidence interval; DM = diabetes mellitus; DR = diabetic retinopathy; HbA1c = hemoglobin A1c; NPDR = nonproliferative diabetic retinopathy; PDR = proliferative diabetic retinopathy; SD = standard deviation.

Table 3. Origin of Retinal Neovascularization

	Retinal Vein	IRMA	Nondilated Capillaries	All
Baseline visit				
RNV sprout, n	14	22	2	38
RNV frond, n	20	2	4	26
Final visit				
RNV sprout, n	16	28	9	53
RNV frond, n	23	3	4	30

IRMA = intraretinal microvascular abnormalities; RNV = retinal neovascularization.

diagnosis of RNV sprouts and RNV fronds (ICC for RNV sprouts, 0.96; ICC for RNV fronds, 0.99).

Longitudinal Observation of RNV Sprout and RNV Fronds

In the 20 eyes with RNV, 64 RNV lesions were identified at the baseline, of which 38 were RNV sprouts and 26 were RNV fronds. When we assessed the origin of the flow signal in the RNV lesions, 34 (53%) originated from veins, 24 (38%) were from IRMA (dilated capillary), and 6 (9%) were from a nondilated capillary bed (Table 3). There was a significant difference in the proportion of origin of RNV between RNV sprouts and RNV fronds at the baseline ($P < 0.001$, Fisher exact test). Twenty-two (58%) RNV sprouts originated from IRMA, but only 2 (8%) RNV fronds were observed at the location of IRMA, and most RNV fronds (77%) originated from retinal veins. The number of RNV sprouts was greater in the treatment-naive eyes than in previously treated eyes (mean [SD] number of RNV sprouts, 2.7 [2.7] vs. 0.7 [0.5]; $P = 0.037$ by unpaired t test), but the number of RNV fronds was similar between the groups (mean [SD] number of RNV fronds, 1.4 [2.9] vs. 1.1 [1.3]; $P = 0.81$ by unpaired t test).

At the final visit, 83 RNV lesions were detected, of which 53 were RNV sprouts, and 30 were RNV fronds. Ten eyes (50%) showed progression of RNV, defined as a new RNV lesion or the development of RNV frond from an RNV sprout. During the follow-up, 4 (11%) of 38 RNV sprouts developed into RNV fronds with intervals ranging from 3 to 10 months (mean [SD], 7.0 [3.6] months). Three RNV fronds that developed during the follow-up originated from retinal veins, and 1 was from IRMA. Although 19 new RNV sprouts formed *de novo* during the follow-up period, no RNV frond developed outside an identified RNV sprout. The proportion of the origin of RNV flow signals at the final visit was similar to those at the baseline (Table 3). Table 4 summarizes the characteristics of the patients with evolution in their RNV.

Comparing the eyes with and without progression, the eyes with progression were younger in age (mean [SD] years, 47.0 [10.3] vs. 59.9 [10.9]; $P = 0.014$ by unpaired t test) and tended to be treatment naive (8 eyes [80%] vs. 3 eyes previously treated [30%], $P = 0.07$ by Fisher exact test) compared with eyes without progression, but there were no differences in other factors including the follow-up duration ($P = 0.33$) and the number of visits ($P = 0.86$; Table 5). There were also no differences in HbA1c (mean [SD] %, 8.6 [3.0] vs. 7.3 [1.3], $P = 0.21$ by unpaired t test) and duration of DM (mean [SD] years, 22.2 [7.3] vs. 21.2 [16.4], $P = 0.86$ by unpaired t test).

Case Presentation

Figures 4, 5, and 6 illustrate the representative cases. Figure 4 (patient number 8) shows a scan superior to the macula from a 51-year-old, treatment-naive, male patient with severe NPDR diagnosis at the initial visit. The *en face* OCT revealed multiple foci of EHM with flow signal seen above the ILM in the corresponding cross-sectional OCTA. These lesions were classified as RNV sprouts. At 10 months, 1 RNV sprout, indicated with a blue arrow, increased in size and developed into a RNV frond that extended into the vitreous cavity. Another RNV sprout, shown with a yellow arrow, increased in size, but the *en face* OCTA did not demonstrate a detectable vascular structure. During the 10-month interval period, this eye received 2 anti-VEGF injections for diabetic macular edema.

Figure 5 (patient number 10) is a scan that includes the optic nerve from a 43-year-old female patient with a PDR diagnosis at baseline. The patient was treatment naive and had no treatment during the follow-up period. At baseline, *en face* OCT revealed a small EHM at the optic disc and a questionable EHM on a superonasal arcade vessel. Flow signals were detected in the EHM at the optic disc on both *en face* OCTA and cross-sectional OCTA. Along a superonasal vessel, a small focus of EHM, indicated with a yellow arrow, with flow signal above the ILM on cross-sectional OCTA is present. This is distinct from other smaller hyperreflective dots seen on the *en face* OCT, which lack flow signal and are similar to previous descriptions of the macrophage-like cell (hyalocyte-like cell).[24–26] Three months later, the RNV sprout at the optic disc developed into recognizable neovascularization at the disc (blue arrow) on *en face* OCTA, continuing to enlarge at 10 months. The EHM seen along the superonasal vessel also increased in size with the detectable flow on *en face* OCTA at 3 months. At 10 months, the lesion developed into a recognizable RNV frond.

Figure 6 (patient number 1) shows the superior scan of a 31-year-old female treatment-naive patient diagnosed with PDR at the initial visit. The eye underwent PRP at 10 months. At the 13-month visit, a focal dilation of the capillary was seen on the *en face* OCTA (white arrow) at the location where no abnormalities in any of the modalities at baseline. At 34 months, the corresponding location had a focus of EHM (white arrow) on *en face* OCT with flow signal above the ILM on cross-sectional OCTA, but *en face* OCTA did not illustrate a distinct vascular structure.

Discussion

In this study, we used *en face* OCT, *en face* OCTA, and cross-sectional OCTA to characterize the early signs of RNV in eyes with PDR and NPDR. The combination of *en face* OCT and cross-sectional OCTA showed the RNV

Table 4. Characteristics of the Eyes with Retinal Neovascularization Evolution

Patient	DR Severity	HbA1c, %	Scan Area, mm	Previous Treatment	Observation Period (M)	Baseline			Final Visit			Treatments During the Follow-up
						RNV Sprout	*RNV Frond*	*Total*	*RNV Sprout*	*RNV Frond*	*Total*	
1	PDR	8.3	6 × 15		34	0	0	0	1	0	1	PRP
2	PDR	6.7	6 × 15		16	2	1	3	4	1	5	PRP
3	Severe NPDR	14	17 × 17		11	6	2	8	9	2	11	
4	PDR	6	6 × 15	PRP	6	1	0	1	5	0	5	Anti-VEGF × 3
5	PDR	7.5	6 × 15	Anti-VEGF	12	1	2	3	2	2	4	
6	Moderate NPDR	6.7	17 × 17		16	6	7	13	7	7	14	
7	Severe NPDR	5.5	17 × 17		10	0	0	0	2	0	2	
8	Severe NPDR	13	17 × 17		10	4	0	4	4	1	5	Anti-VEGF × 2
9	PDR	10.9	17 × 17		5	6	1	7	5	2	7	PRP
10	PDR	7.8	17 × 17		11	2	0	2	4	2	6	

DR = diabetic retinopathy; HbA1c = hemoglobin A1c; NPDR = nonproliferative diabetic retinopathy; PDR = proliferative diabetic retinopathy; PRP = panretinal photocoagulation; RNV = retinal neovascularization.

sprout before it can be recognized on *en face* OCTA. Longitudinal observation illustrated that RNV sprouts developed into RNV fronds, suggesting that RNV sprouts may be the early sign of RNV. Prior studies have already reported RNV sprout-like changes at the location of IRMA using SD-OCT and OCTA.[7–10] In the current study, we utilized *en face* OCT that can show structural changes on the entire plane of the retinal surface to identify early initiation of RNV at not only IRMA but also in retinal veins and nondilated capillaries. Thus, combining *en face* OCT and cross-sectional OCTA could be useful to detect the early stages of RNV.

A RNV sprout was seen by cross-sectional OCT as a pyramid-shaped EHM (Figs 3–6). This is similar to the histologic descriptions of autopsy eyes with retinopathy of prematurity[27] and to eyes from experimental nonhuman primates,[28] which were presumed to be early endothelial proliferation. Some of these lesions increased in size on *en face* OCT and became recognizable on *en face* OCTA with characteristic vascular patterns of RNV (Figs 4, 5). Lee et al demonstrated IRMA initially outpouching the ILM without breaching the ILM, subsequently progressing into RNV. Similarly, we also saw that an RNV sprout can evolve from IRMA (Fig 6), seeming to outpouch the ILM (Fig 6F) then breaching the ILM (Fig 6I). However, the case in Figure 5 demonstrated that an RNV sprout (indicated with a yellow arrow) can evolve directly from a retinal vein without an outpouching dilated capillaries. In this study, the RNV originating from IRMA represented 38% of cases, and the other RNV lesions were from retinal veins and nondilated capillaries, consistent with a prior study.[12] Although IRMA could be a precursor of RNV,[7–10] EHM on *en face* OCT also could be an important precursor of RNV associated with an increased risk of progression to PDR.

Prior histological studies showed early structural changes in RNV,[27,28] and foci of the proliferation of both vascular and connective tissues into the vitreous,[29] corresponding to the recent OCT and OCTA findings of early structural changes in proliferative retinal vascular diseases.[7,8,15,30,31] Because differentiation and proliferation of the endothelial cells precede the formation of the vessel lumen,[32] it is not surprising that structural changes can be observed before the flow is detected. Additionally, the structural area of RNV is greater than the flow area of RNV.[33] Therefore, *en face* OCT is a useful method to identify early structural changes in RNV. The flow signal above the ILM detected by cross-sectional OCTA is essential for differentiating RNV sprouts from IRMA and other retinal abnormalities.[34] However, inspecting each B-frame, particularly in a wide-field OCTA, may be impractical in a clinical setting. A single 17 × 17-mm montage scan in this study contains 2400 B-scans. Identifying key areas of interest using the *en face* OCT by recognizing focal EHM may be a useful, expedited way to identify early signs of RNV. Although the *en face* OCT improves the efficiency, reviewing a combination of *en face* OCT, *en face* OCTA, and cross-sectional OCTA for detecting RNV may still be impractical for a real-life clinical setting. An algorithm that can automatically

Table 5. Characteristics of Eyes with and without RNV Progression

Parameters	RNV Progression (+) (n = 10)	RNV Progression (−) (n = 10)	*P* Value
Age, yrs (SD) [95% CI]	47.0 (10.3) [39.7–54.3]	59.9 (10.9) [52.1–67.7]	0.014†
Sex, n (male/female)	6/4	5/5	1.00*
Most recent HbA1c, % (SD) [95% CI]	8.6 (3.0) [6.5–10.8]	7.3 (1.3) [6.4–8.2]	0.21†
Duration of DM, yrs (SD) [95% CI]	22.2 (7.3) [17.0–27.4]	21.2 (16.4) [9.5–32.94]	0.86†
Type 1 DM, n (%)	6 (60)	4 (40)	0.66*
Follow-up duration, mos (SD) [95% CI]	13.1 (8.2) [7.3–18.9]	17.9 (13.0) [8.6–27.2]	0.33†
OCTA scans, n (SD) [95% CI]	3.3 (1.2) [2.5–4.1]	3.4 (1.3) [2.5–4.3]	0.86†
DR stage			
Moderate NPDR, eyes (%)	1 (10.0)	0 (0.0)	1.00*
Severe NPDR, eyes (%)	3 (30.0)	3 (30.0)	
PDR, eyes (%)	6 (60.0)	7 (70.0)	
Treatment naive, eyes (%)	8 (80)	3(30)	0.070*
Treatments during the follow-up, eyes (%)	5 (50)	5 (50)	1.00*

CI = confidence interval; DM = diabetes mellitus; DR = diabetic retinopathy; HbA1c = hemoglobin A1c; NPDR = nonproliferative diabetic retinopathy; PDR = proliferative diabetic retinopathy; SD = standard deviation.
*Fisher exact test.
†Unpaired *t* test.

detect these lesions may be necessary to be able to apply these insights to everyday clinical practice.

In the current study, 4 RNV sprouts developed into RNV fronds with a mean interval of 7 months (range, 3 to 10 months). Prior studies reported that the IRMA progressed into an RNV 1 to 14 months after the initial evaluation. Similarly, ETDRS report No. 9 recommended that the patients with severe NPDR and non–high-risk PDR be examined within 2 to 4 months because the risk of progression to PDR was high,[35] suggesting the RNV development from RNV sprouts and IRMA may occur within a few months. The combination of *en face* OCT

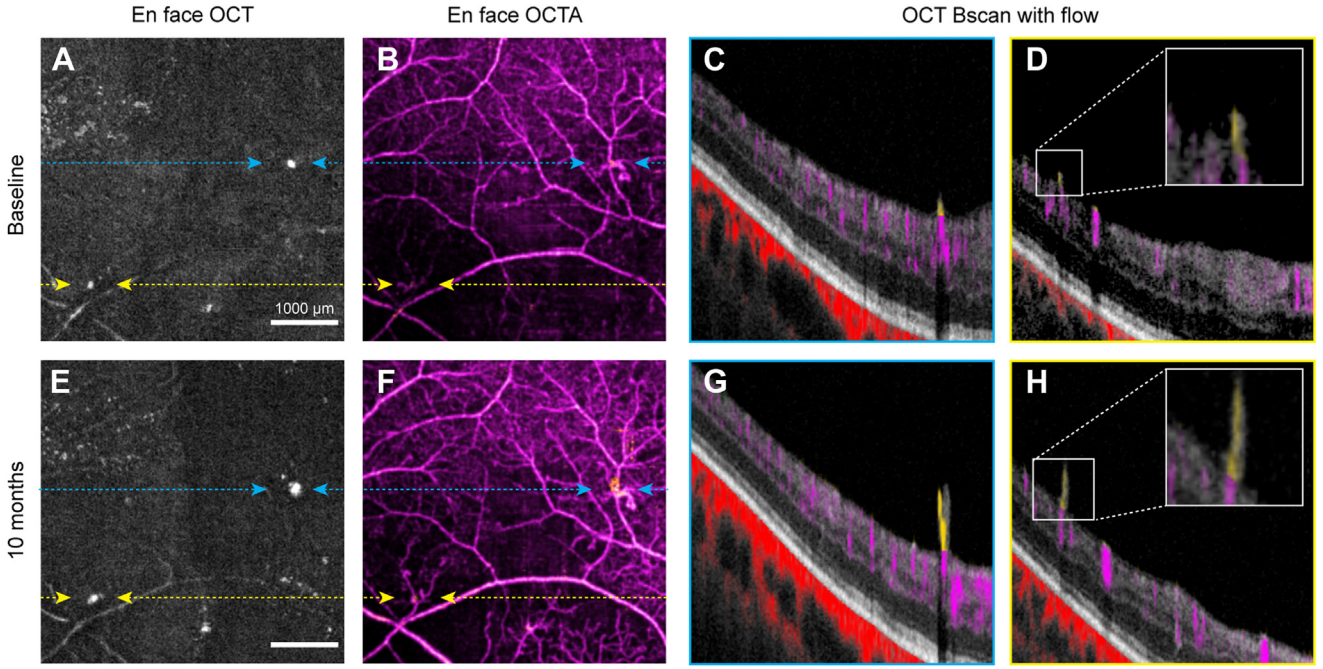

Figure 4. Representative case from a 51-year-old treatment-naive male patient with severe nonproliferative diabetic retinopathy. The baseline *en face* OCT (**A**) showed retinal neovascularization (RNV) sprouts (blue and yellow dashed arrows) as hyperreflective foci which have flow signal above the internal limiting membrane on corresponding cross-sectional OCT angiography (OCTA) (**C** and **D**, respectively) but are difficult to recognize as RNV on *en face* OCTA (**B**). At 10 months, these hyperreflective foci increased in area on *en face* OCT (**E**) and in height on the cross-sectional OCTA (**G**). One RNV sprout (blue dashed arrow) formed a recognizable vascular pattern and was classified into an RNV frond (forward type), whereas the other (yellow dashed arrow) remained indistinct on *en face* OCTA (**B**) and was classified as an RNV sprout.

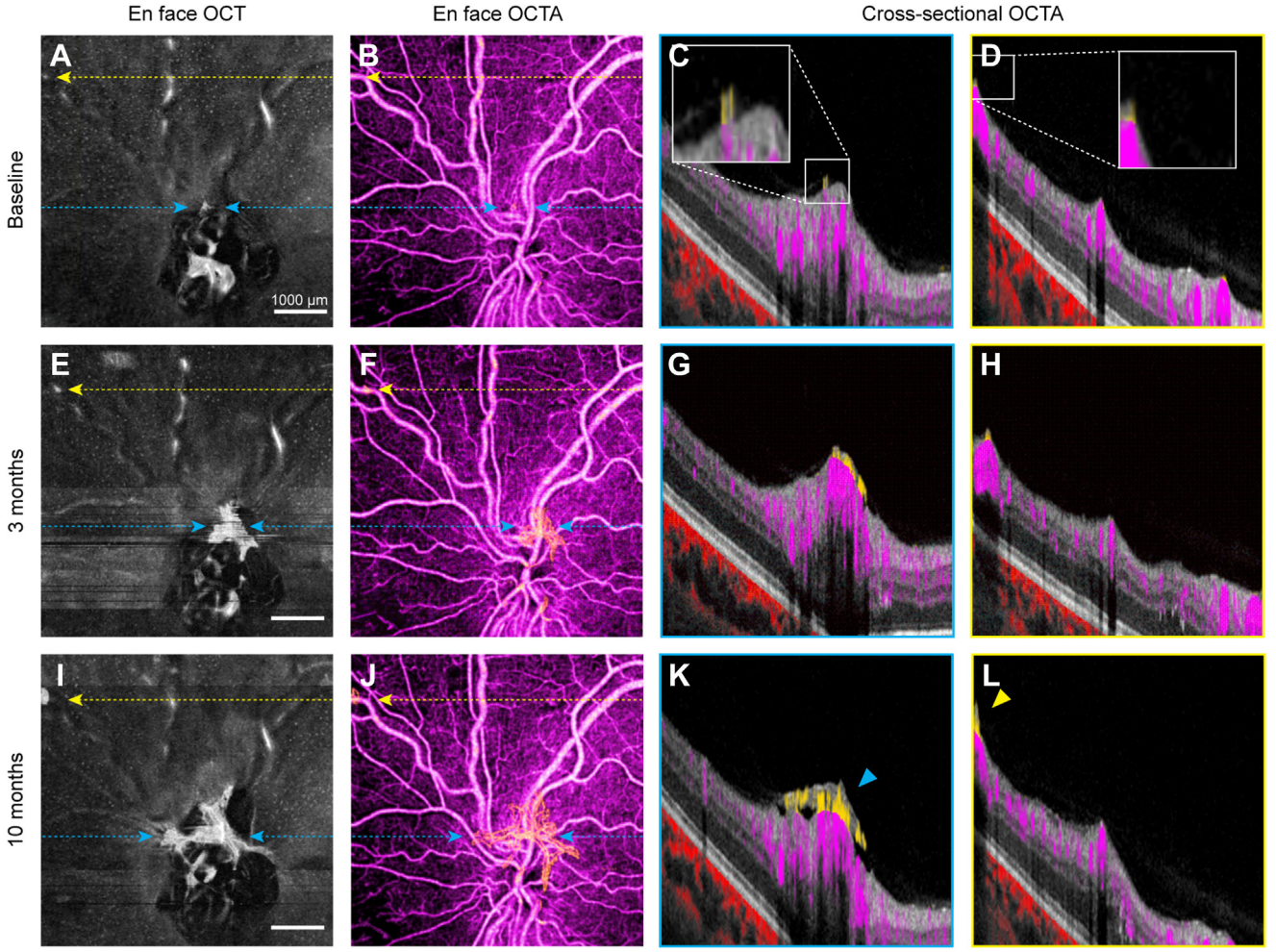

Figure 5. Representative case from a 43-year-old female patient with a proliferative diabetic retinopathy diagnosis at baseline. The baseline *en face* OCT (**A**) showed epiretinal hyperreflective material (EHM) on the optic disc (blue dashed arrow) and questionable EHM on the superonasal vessel (yellow dashed arrow). Corresponding cross-sectional OCT angiography (OCTA) images (**C, D**) show small tissue above the internal limiting membrane with flow signal. At 3 months, the lesion on the optic disc was clearly recognizable as retinal neovascularization frond on *en face* OCTA (**F**) and further increased in size at 10 months (**J**). On *en face* OCT (**E, I**), the small superonasal lesion (yellow dashed arrow) also grew in size and was recognizable as a vascular loop at 10 months on *en face* OCTA (**J**). Note that the EHM at the inferior optic disc on *en face* OCT (**A, E, I**) is an artifact due to a segmentation error.

and OCTA illustrated the sequential process of RNV; however, we could not find the relationship between RNV and other preretinal findings such as macrophage-like cells (hyalocyte-like cells)[24–26] and epivascular glia.[36] A more frequent observation may be necessary to elucidate the spatial relationship between these preretinal cells and RNV evolution.

In this cohort, the treatment-naive eyes had more RNV sprouts and tended to have more progression over the follow-up period, suggesting that treatment has an effect on the development of early RNV. However, although recent randomized clinical trials demonstrated that anti-VEGF treatment lowers the probability of eyes with moderate-to-severe NPDR progressing to PDR, it did not change the visual outcome or the rate of vitreous hemorrhage from PDR.[37–40] But these studies included eyes with moderate-to-severe NPDR, many of which do not progress to PDR. It is possible that by identifying the subgroup of patients with unrecognized RNV lesions, including RNV sprouts and subclinical RNV fronds, a clinical diagnosis of moderate-to-severe NPDR could make a meaningful difference in the visual outcome while reducing the population treatment burden. Further study that pairs treatment with early detection is necessary to test whether this approach can improve outcomes for patients with DR.

It should be noted that OCTA was essential in confirming the nature of the epiretinal lesions in this study. Lee et al demonstrated the utility of structural OCT in evaluating IRMA and neovascularization, pointing to the histological aspects that OCT B-scan can reveal that fluorescein angiography (FA) cannot.[7] They also included cases that were diagnosed as RNV by clinical examination and by OCT but lacked leakage on FA and further argued that FA is a useful but not definitive tool in determining whether a lesion was NV elsewhere. Furthermore, they recognized that there were cases with disagreement between clinical

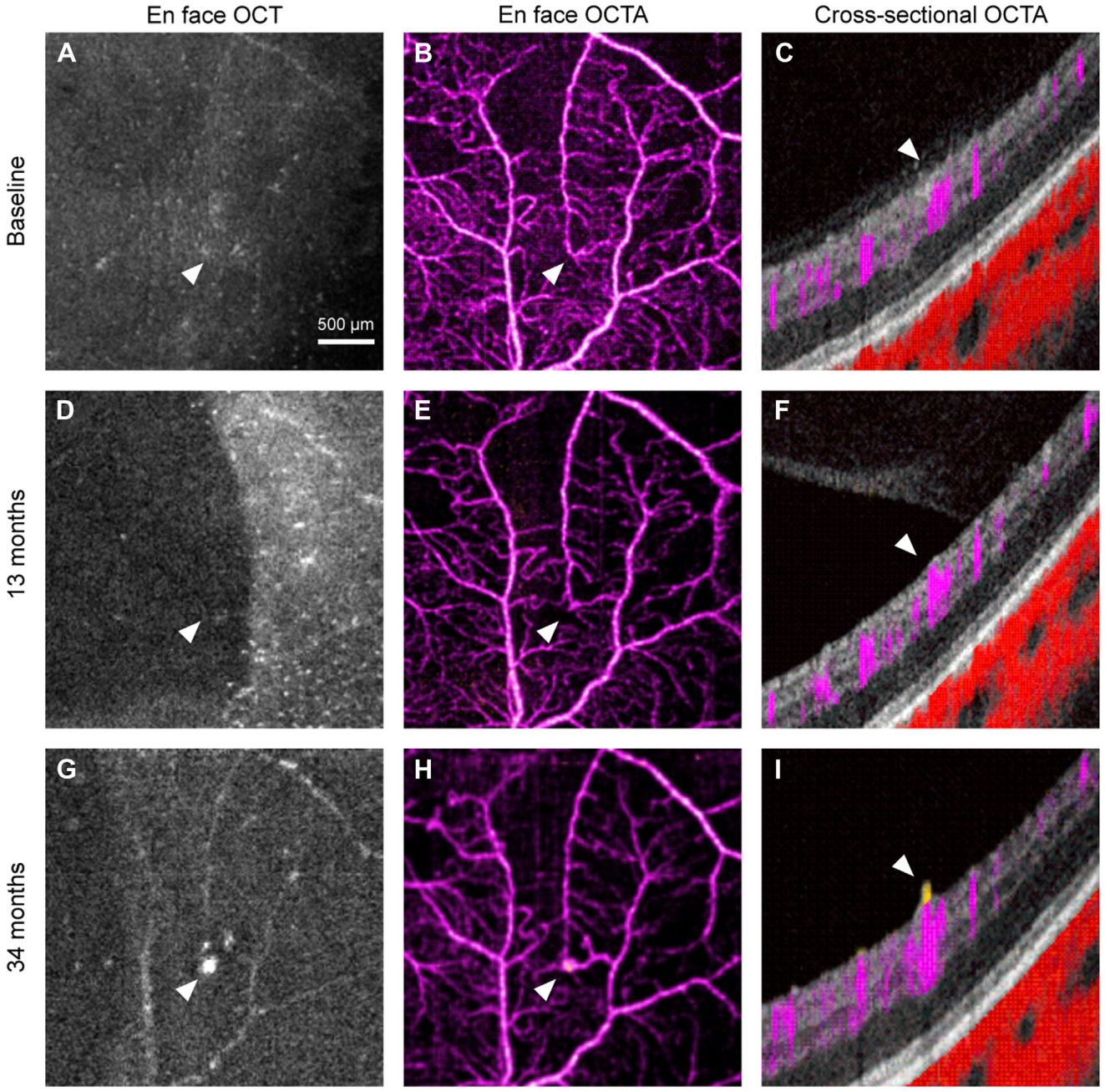

Figure 6. The progression of a retinal vascularization sprout from an intraretinal microvascular abnormality (IRMA). **A–C,** no abnormalities are observable at the baseline by any image modalities. At 13 months, *en face* OCT angiography (OCTA) (**E**) showed an IRMA where no abnormalities were observed at baseline. At 34 months, both epiretinal hyperreflective material on *en face* OCT (**G**) and IRMA on *en face* OCTA (**H**) showed increase in size, and cross-sectional OCT (I) showed the breaching of the internal limiting membrane.

examination and structural OCT findings in determining whether a lesion was IRMA or RNV. For these, the technology at the time (2012–2013) did not offer a way to determine the nature of the lesion. With OCTA, however, the ability to see flow signal above the ILM allows for a more satisfactory way to classify a lesion that correlates to histology than clinical examination, FA, or structural OCT.

There are several limitations to this study. The study was retrospective with a small number of patients. Visit intervals and treatment protocol were not standardized. The goal of treatment with anti-VEGF injections in this cohort was to manage diabetic macular edema or clinically evident PDR not necessarily for preventing or eliminating all RNV lesions. The clinicians did not have access to the images that demonstrated the subclinical

RNV. It is perhaps not surprising that the treatment did not necessarily correlate to lower incidence or area of RNV lesions. Although HbA1c and DM duration were well-known risk factors for worsening DR,[2] they were not correlated with the progression of RNV in this study. Because the small sample size limits analysis, further study with a large sample size is needed. The study included 2 different OCTA scan protocols with different fields of view. Although all scans had the same sampling density (15 μm/A-line), different scan areas affected the detection rate of RNV sprouts and RNV fronds. We did not differentiate IRMA with outpouching the ILM from the IRMA with breaching the ILM proposed by Lee et al,[7] because our imaging protocol did not have an adequate resolution. Instead, we used a combination of structural and angiographic images to distinguish IRMA from RNV. Most RNV lesions are located in the midperipheral retina at a distance of 1 to 6 disc diameters away from the disc margin.[41] A 15- × 9-mm montaged OCTA is expected to detect only 39.0% of RNV lesions detected by ultra-widefield FA.[42] Although the aim of the study was not to assess the sensitivity of this technique to detect RNV lesions, we likely have missed many RNV lesions due to the limited field of view. Additionally, the study documented the development of RNV sprouts into RNV fronds; however, it is unknown whether an earlier detection and treatment of these subclinical lesions can reduce the risk of vision-threatening complications, such as vitreous hemorrhage and tractional retinal detachment.

In conclusion, we have demonstrated that a combination of *en face* OCT, *en face* OCTA, and cross-sectional OCTA can reveal the early stages of RNV before they are clinically recognizable. Longitudinal observation demonstrated that RNV sprouts develop into RNV fronds, suggesting that RNV sprouts may be an early sign of RNV evolution. Hyperreflective foci on the *en face* OCT could be a biomarker for early detection of PDR.

Footnotes and Disclosures

Originally received: February 28, 2023.
Final revision: June 12, 2023.
Accepted: August 7, 2023.
Available online: August 13, 2023. Manuscript no. XOPS-D-22-00266R1.

[1] Casey Eye Institute, Oregon Health and Science University, Portland, Oregon.

[2] Department of Ophthalmology, Aichi Medical University, 1-1, Yazako-Karimata, Nagakute, Aichi, 480-1195, Japan.

[3] Department of Biomedical Engineering, Oregon Health & Science University, Portland, Oregon.

Presented at the ARVO meeting 2023 in New Orleans, paper session.

Disclosures:
All authors have completed and submitted the ICMJE disclosures form.

The authors have made the following disclosures: J.W.: Financial interest − Optovue/Visionix Inc.

Y.J.: Financial interest − Optovue/Visionix Inc.

D.H.: Financial interest − Optovue/Visionix Inc.; Consultant − Boeringer Ingelheim.

K.T.: Financial interest − Bayer, Santen, Chugai, Alcon, Senju.

None of the other authors have any proprietary or commercial interest in any materials discussed in this article.

This work was supported by the National Institute of Health (R01 EY035410, R01 EY027833, R01 EY024544, R01 EY031394, T32 EY023211, UL1TR002369, P30 EY010572); the Malcolm M. Marquis, MD Endowed Fund for Innovation; an Unrestricted Departmental Funding Grant and Dr H. James and Carole Free Catalyst Award from Research to Prevent Blindness (NewYork, NY), Edward N. & Della L. Thome Memorial Foundation Award, and the Bright Focus Foundation (G2020168, M20230081). The funding source had no role in the design and conduct of the study; collection, management, analysis, and interpretation of the data; preparation, review, or approval of the manuscript; and decision to submit the manuscript for publication.

This research was presented at the ARVO meeting, April 23−27, New Orleans, LA.

HUMAN SUBJECTS: Human subjects were included in this study. The study adhered to the tenets of the Declaration of Helsinki and complied with the Health Insurance Portability and Accountability Act of 1996. The institutional review board of Oregon Health Science University approved the study. All participants provided a written informed consent to participate in the OCT/OCT angiography studies.

No animal subjects were included in this study.

Author Contributions:

Conception and design: Tsuboi, Hwang

Data collection: Tsuboi, Mazloumi, Flaxel, Bailey, Hwang

Analysis and interpretation: Tsuboi, Guo, Wang, Jia, Hwang

Obtained funding: Jia, Hwang

Overall responsibility: Tsuboi, Wilson, Huang, Jia, Hwang

Abbreviations and acronyms:
CI = confidence interval; **DR** = diabetic retinopathy; **EHM** = epiretinal hyperreflective material; **ICC** = interclass correlation coefficient; **ILM** = internal limiting membrane; **IRMA** = intraretinal microvascular abnormality; **NPDR** = nonproliferative diabetic retinopathy; **NVD** = neovascularization of the disc; **PDR** = proliferative diabetic retinopathy; **OCTA** = OCT angiography; **RNV** = retinal neovascularization; **SD** = standard deviation.

Keywords:
Proliferative diabetic retinopathy, En face OCT, OCT angiography, Retinal neovascularization, Retinal neovascularization sprout.

Correspondence:
Thomas S. Hwang, Casey Eye Institute, Oregon Health & Science University, 515 SW Campus Dr, Portland, OR 97239. E-mail: hwangt@ohsu.edu.

References

1. Cheung N, Mitchell P, Wong TY. Diabetic retinopathy. *Lancet*. 2010;376:124−136.
2. Yau JW, Rogers SL, Kawasaki R, et al. Global prevalence and major risk factors of diabetic retinopathy. *Diabetes Care*. 2012;35:556−564.
3. Tan GS, Cheung N, Simó R, et al. Diabetic macular oedema. *Lancet Diabetes Endocrinol*. 2017;5:143−155.
4. Wong TY, Sun J, Kawasaki R, et al. Guidelines on diabetic eye care: the International Council of Ophthalmology recommendations for screening, follow-up, referral, and treatment based on resource settings. *Ophthalmology*. 2018;125:1608−1622.
5. Fundus photographic risk factors for progression of diabetic retinopathy. ETDRS report number 12. Early Treatment Diabetic Retinopathy Study Research Group. *Opthalmology*. 1991;98:823−833.
6. Early Treatment Diabetic Retinopathy Study design and baseline patient characteristics. ETDRS report number 7. *Opthalmology*. 1991;98:741−756.
7. Lee CS, Lee AY, Sim DA, et al. Reevaluating the definition of intraretinal microvascular abnormalities and neovascularization elsewhere in diabetic retinopathy using optical coherence tomography and fluorescein angiography. *Am J Opthalmol*. 2015;159:101−110.e1.
8. Russell JF, Shi Y, Scott NL, et al. Longitudinal angiographic evidence that intraretinal microvascular abnormalities can evolve into neovascularization. *Ophthalmol Retina*. 2020;4:1146−1150.
9. Shimouchi A, Ishibazawa A, Ishiko S, et al. A proposed classification of intraretinal microvascular abnormalities in diabetic retinopathy following panretinal photocoagulation. *Invest Opthalmol Vis Sci*. 2020;61:34. https://doi.org/10.1167/iovs.61.3.34.
10. Ishibazawa A, Nagaoka T, Takahashi A, et al. Optical coherence tomography angiography in diabetic retinopathy: a prospective pilot study. *Am J Opthalmol*. 2015;160:35−44.e1.
11. Wise GN. Retinal neovascularization. *Trans Am Opthalmol Soc*. 1956;54:729−826.
12. Pan J, Chen D, Yang X, et al. Characteristics of neovascularization in early stages of proliferative diabetic retinopathy by optical coherence tomography angiography. *Am J Opthalmol*. 2018;192:146−156.
13. Pan J, Chen F, Chen D, et al. Novel three types of neovascularization elsewhere determine the differential clinical features of proliferative diabetic retinopathy. *Retina*. 2021;41:1265−1274.
14. Norton EW, Gutman F. Diabetic retinopathy studied by fluorescein angiography. *Trans Am Opthalmol Soc*. 1965;63:108−128.
15. Tsuboi K, Ishida Y, Wakabayashi T, Kamei M. Presumed glial sprouts as a predictor of preretinal neovascularization in retinal vein occlusion. *JAMA Ophthalmol*. 2022;140:284−285.
16. Hwang TS, Gao SS, Liu L, et al. Automated quantification of capillary nonperfusion using optical coherence tomography angiography in diabetic retinopathy. *JAMA Ophthalmol*. 2016;134:367−373.
17. Hwang TS, Hagag AM, Wang J, et al. Automated quantification of nonperfusion areas in 3 vascular plexuses with optical coherence tomography angiography in eyes of patients with diabetes. *JAMA Ophthalmol*. 2018;136:929−936.
18. You QS, Tsuboi K, Guo Y, et al. Comparison of central macular fluid volume with central subfield thickness in patients with diabetic macular edema using optical coherence tomography angiography. *JAMA Ophthalmol*. 2021;139:734−741.
19. You QS, Wang J, Guo Y, et al. Optical Coherence Tomography Angiography Avascular Area Association With 1-Year Treatment Requirement and Disease Progression in Diabetic Retinopathy. *Am J Ophthalmol*. 2020;217:268−277.
20. Tsuboi K, You QS, Guo Y, et al. Association between fluid volume in inner nuclear layer and visual acuity in diabetic macular edema. *Am J Ophthalmol*. 2022;237:164−172.
21. Russell JF, Shi Y, Hinkle JW, et al. Longitudinal wide-field swept-source OCT angiography of neovascularization in proliferative diabetic retinopathy after panretinal photocoagulation. *Ophthalmol Retina*. 2019;3:350−361.
22. Hirano T, Hoshiyama K, Hirabayashi K, et al. Vitreoretinal interface slab in OCT angiography for detecting diabetic retinal neovascularization. *Ophthalmol Retina*. 2020;4:588−594.
23. Schwartz R, Khalid H, Sivaprasad S, et al. Objective evaluation of proliferative diabetic retinopathy using OCT. *Ophthalmol Retina*. 2020;4:164−174.
24. Castanos MV, Zhou DB, Linderman RE, et al. Imaging of macrophage-like cells in living human retina using clinical OCT. *Invest Ophthalmol Vis Sci*. 2020;61:48. https://doi.org/10.1167/iovs.61.6.48.
25. Migacz JV, Otero-Marquez O, Zhou R, et al. Imaging of vitreous cortex hyalocyte dynamics using non-confocal quadrant-detection adaptive optics scanning light ophthalmoscopy in human subjects. *Biomed Opt Express*. 2022;13:1755−1773.
26. Ong JX, Nesper PL, Fawzi AA, et al. Macrophage-like cell density is increased in proliferative diabetic retinopathy characterized by optical coherence tomography angiography. *Invest Ophthalmol Vis Sci*. 2021;62:2. https://doi.org/10.1167/iovs.62.10.2.
27. Reese AB, Blodi FC, Locke JC. The pathology of early retrolental fibroplasia, with an analysis of the histologic findings in the eyes of newborn and stillborn infants. *Am J Ophthalmol*. 1952;35:1407−1426.
28. Tolentino MJ, McLeod DS, Taomoto M, et al. Pathologic features of vascular endothelial growth factor-induced retinopathy in the nonhuman primate. *Am J Ophthalmol*. 2002;133:373−385.
29. Faulborn J, Bowald S. Microproliferations in proliferative diabetic retinopathy and their relationship to the vitreous: corresponding light and electron microscopic studies. *Graefes Arch Clin Exp Ophthalmol*. 1985;223:130−138.
30. Chen X, Mangalesh S, Dandridge A, et al. Spectral-domain OCT findings of retinal vascular-avascular junction in infants with retinopathy of prematurity. *Ophthalmol Retina*. 2018;2:963−971.
31. Muqit MM, Stanga PE. Fourier-domain optical coherence tomography evaluation of retinal and optic nerve head neovascularisation in proliferative diabetic retinopathy [published correction appears in Br J Opthalmol. 2014;98:713] *Br J Opthalmol*. 2014;98:65−72.

32. Campochiaro PA. Ocular neovascularization. *J Mol Med (Berl)*. 2013;91:311–321.
33. Tsuboi K, Mazloumi M, Guo Y, et al. Utility of en face OCT for the detection of clinically unsuspected retinal neovascularization in patients with diabetic retinopathy. *Opthalmol Retina*. 2023;7:683–691.
34. Arya M, Sorour O, Chaudhri J, et al. Distinguishing intraretinal microvascular abnormalities from retinal neovascularization using optical coherence tomography angiography. *Retina*. 2020;40:1686–1695.
35. Early Treatment Diabetic Retinopathy Study Research Group. Early photocoagulation for diabetic retinopathy. ETDRS report number 9. *Opthalmology*. 1991;98:766–785.
36. Grondin C, Au A, Wang D, et al. Identification and characterization of epivascular glia using en face optical coherence tomography. *Am J Opthalmol*. 2021;229:108–119.
37. Mitchell P, McAllister I, Larsen M, et al. Evaluating the impact of intravitreal aflibercept on diabetic retinopathy progression in the VIVID-DME and VISTA-DME studies. *Ophthalmol Retina*. 2018;2:988–996.
38. Brown DM, Wykoff CC, Boyer D, et al. Evaluation of intravitreal aflibercept for the treatment of severe nonproliferative diabetic retinopathy: results from the PANORAMA randomized clinical trial. *JAMA Ophthalmol*. 2021;139:946–955.
39. Wykoff CC, Eichenbaum DA, Roth DB, et al. Ranibizumab induces regression of diabetic retinopathy in most patients at high risk of progression to proliferative diabetic retinopathy. *Opthalmol Retina*. 2018;2:997–1009.
40. Maturi RK, Glassman AR, Josic K, et al. Effect of intravitreous anti-vascular endothelial growth factor vs sham treatment for prevention of vision-threatening complications of diabetic retinopathy: the protocol W randomized clinical trial. *JAMA Ophthalmol*. 2021;139:701–712.
41. Shimizu K, Kobayashi Y, Muraoka K. Midperipheral fundus involvement in diabetic retinopathy. *Ophthalmology*. 1981;88:601–612.
42. Zhu Y, Cui Y, Wang JC, et al. Different scan protocols affect the detection rates of diabetic retinopathy lesions by wide-field swept-source optical coherence tomography angiography. *Am J Opthalmol*. 2020;215:72–80.